Monograph:
Tokhi, O. and Leitch, R.R. (1991) Design of Active Noise Control Systems Operating in Three-Dimensional Nondispersive Propagation Medium. Research Report. Acse Report 425 . Dept of Automatic Control and System Engineering. University of Sheffield

Design of active noise control systems operating in three–dimensional nondispersive propagation medium

M O Tokhi * and R R Leitch **

* The University of Sheffield,
Department of Control Engineering,
Mappin Street,
Sheffield S1 3JD, U.K.

** Heriot-Watt University,
Department of Electrical and Electronic Engineering,
31-35 Grassmarket,
Edinburgh EH1 2HT, U.K.

Research Report No. 425

May 1991

Table of contents

Abstract

A coherent method for the design of active noise control (ANC) systems operating in a three-dimensional non-dispersive propagation medium (acoustic free field) is presented. An analysis of the basic control structures is provided and conditions for the robust operation of such systems are determined. Finally these conditions are interpreted as constraints on the geometric compositions of the ANC system.

1. Introduction

Active noise control uses the intentional superposition of acoustic waves to create a destructive interference pattern such that a reduction of the unwanted sound occurs. This is realised by a single or a number of secondary (cancelling) sources of sound, driven by electrical signals derived from the primary (unwanted) noise through detection sensors and then passed through an electronic controller, so that when the secondary wave is superimposed on the primary wave the two destructively interfere and reduction of the sound occurs. It follows from the above that, from a practical point of view, the active attenuation (or cancellation) of an unwanted sound wave through wave interference consists of the three main processes of detection, negation and superposition.

In the process of detection the main aim is to obtain a signal coherent with the unwanted noise over the frequency range of interest. In this case, the device to be used as a detector is required to have a suitable response characteristic to provide this information. Microphones which have a reasonably flat amplitude and a linear phase characteristic, are commonly used as detectors. Here the detector is placed at a fixed distance relative to the source of noise (primary source) in which case the amplitude and phase of the noise signal will, before detection, be altered due to the acoustic properties of the space between the primary source and the detector.

An alternative to direct detection is to detect unwanted noise through obtaining a non-acoustic signal that is coherent with the primary source noise [1-4]. Many sources of noise, for instance, vibrate continuously when in operation and the vibration is found to be coherent with the acoustic waves they emit. In these circumstances vibration-sensitive devices can be used as detectors. Flame noise is another example where the coherence between light and noise has been found to be as much as 99% [2, 4]. An advantage of indirect detection is that acoustic feedback that can sometimes lead to problems of instability, is avoided. However, indirect detection must be used with care to ensure that a good measure of the noise is obtained.

The most important part, and the main body of ANC, is the process of negation of the signal. The device performing this task (the controller) should be capable of not only adjusting the amplitude but also shifting the phase of each frequency component of the detected signal, accordingly, by 180° relative to the primary wave. The controller is, therefore, defined by a continuous transfer function representing the required amplitude and phase characteristics. Thus, when the processed wave emitted by the secondary source is superimposed on the primary wave destructive interference results. The required controller characteristics are dependent upon the characteristics of the transmission paths from the primary and secondary sources to the detection and observation points as well as the characteristics of the secondary source and transducers used in the system. Therefore, the measurement of these characteristics is essential in obtaining a suitable controller.

After the detected signal has been processed by the controller, the output of the controller is used to drive the secondary source. This leads to an acoustic wave that interacts with the acoustic wave from the primary source. Here a loudspeaker placed at a set distance from the primary source can be used as a secondary source. The result of superimposing the component waves can be observed by using an observer microphone. From the above discussion it follows that processes of detection and superposition are relatively straightforward whereas the main task in active noise control is the design of a suitable controller.

This report presents a coherent method for the design of ANC systems operating in a three-dimensional non-dispersive propagation medium. An analysis of the basic control structures; namely, feedback control and feedforward control is presented and conditions for the robust performance of such systems are determined. The resulting controller design equations are then related to the system geometry. Using such a relation and the acoustic properties of the medium as mapped onto, say, pressure fluctuations due to a sound wave, which in this case vary in amplitude inversely with distance from the source and in phase directly with the product of frequency and distance from the source, the above conditions are interpreted as constraints on the geometric composition of the ANC system.

2. Active noise control structures

Active noise control requires a suitable interconnection of detector, controller and secondary source. The various arrangements of detector(s), controller and secondary source(s) in single/multiple detector and/or source configurations have resulted in various control structures for ANC systems. These structures can be classified into two basic types: feedback control and feedforward control.

2.1. *Feedback control structure*

The geometric arrangement of the feedback control structure (FBCS) is shown schematically in Fig. 1a. The primary source emits a wave $p(t)$. This is detected by a transducer (detector), placed at a fixed distance relative to the primary source, and passed to a controller C. The controller is required to adjust the phase as well as the amplitude of each

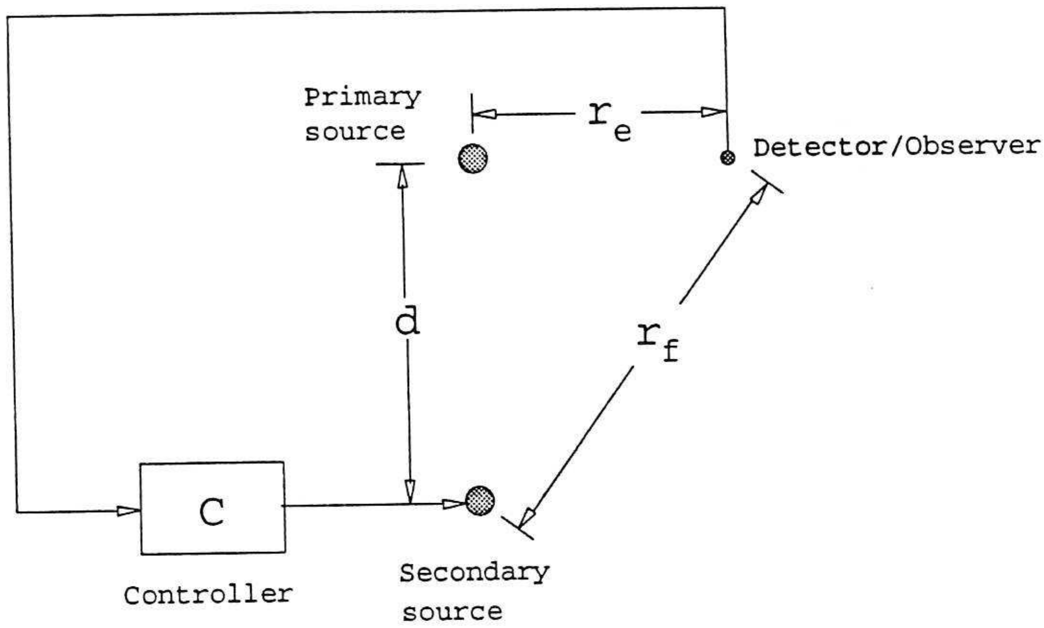

(a)

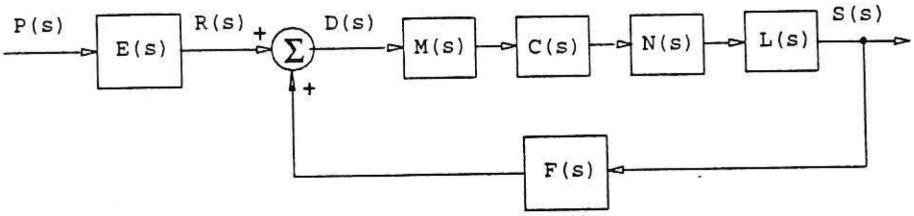

(b)

Fig. 1: Feedback control structure;

(a) Schematic diagram,

(b) Block diagram.

frequency component contained in the detected signal such that when emitted by the secondary source a zero sound pressure level results at the detector location. Hence, the detector can at the same time be an observer.

A block diagram of the FBCS in the complex frequency s domain is shown in Fig. 1b, where

$E(s)$ = transfer function of acoustic path between primary source and detector,

$F(s)$ = transfer function of acoustic path between secondary source and detector,

$M(s)$ = transfer function of detector,

$C(s)$ = transfer function of controller,

$N(s)$ = transfer function of necessary electronics, in addition to the controller,

$L(s)$ = transfer function of secondary source.

Fig. 1b clearly shows the feedback nature of the structure; a (control) signal $S(s)$ is emitted by the secondary source that is fed back to the detector, through the acoustic transmission path between the secondary source and detector, where it adds to a (reference) signal $R(s)$ to produce a (residual or error) signal $D(s)$. The detector signal $D(s)$ can be written as

$$D(s) = R(s) + F(s)S(s)$$

or

$$D(s) = E(s)P(s) + F(s)M(s)C(s)N(s)L(s)D(s)$$

Thus, the above, after simplification, yields the transfer function between the detector signal $D(s)$ and the primary source signal $P(s)$ as

$$\frac{D(s)}{P(s)} = \frac{E(s)}{1 - M(s)C(s)N(s)L(s)F(s)} \quad (1)$$

Assuming the controller always reverses the polarity of the signal, equation (1) can thus be written as

$$\frac{D(s)}{P(s)} = \frac{E(s)}{1 + M(s)C'(s)N(s)L(s)F(s)} \tag{2}$$

where $C'(s) = -\,C(s)$. Equation (2) corresponds to a standard negative feedback structure.

The FBCS corresponds to that proposed by Lueg in his patent where the controller is realised by an electronic transmission line providing a constant time delay and hence phase inversion of a single frequency [5]. Similarly, Olson employed the FBCS in his electronic sound absorber with an amplifier as a controller, providing only gain adjustment and no frequency compensation adjustment [6-8]. Following Olson's work a significant amount of consideration has been given to the investigation and performance improvement of this structure in various applications [9-13.

2.2. *Feedforward control structure*

A schematic diagram of the geometric arrangement of the feedforward control structure (FFCS) is shown in Fig. 2a. The primary source emits a wave $p(t)$. This is detected by a detector placed at a distance r_e relative to the primary source and a distance r_f relative to the secondary source and passed to the controller C. After the detected signal has been adjusted in phase and amplitude it is emitted by the secondary source to be superimposed on the unwanted noise. The result of this superposition is observed at an observation point located at a distance r_g relative to the primary source and a distance r_h relative to the secondary source.

A block diagram of Fig. 2a in the complex frequency s domain is shown in Fig. 2b, where

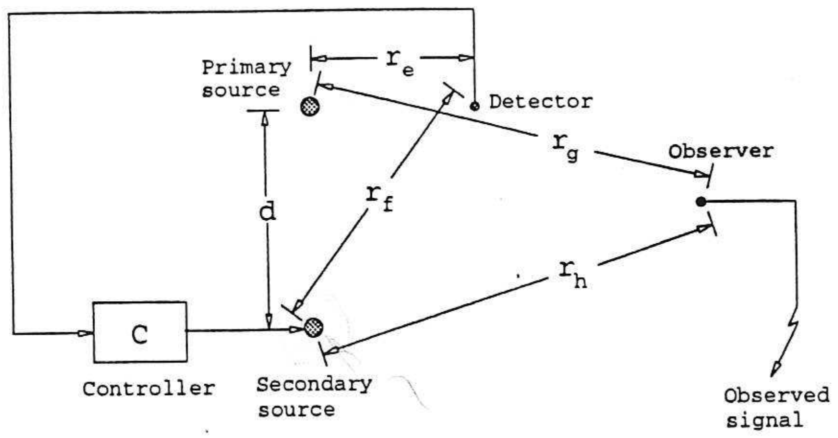

(a)

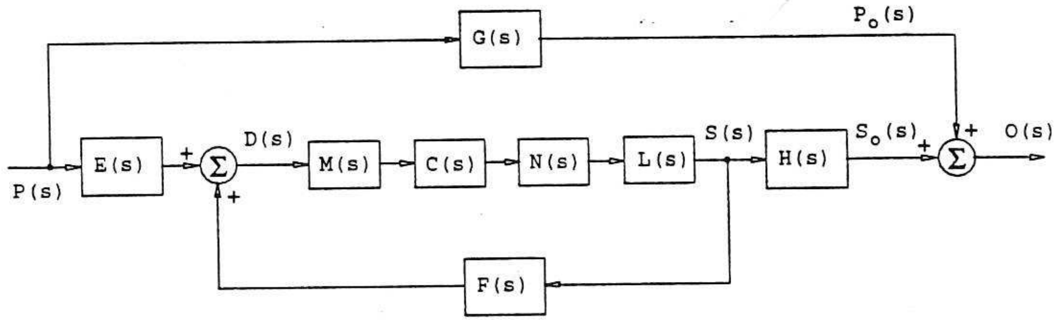

(b)

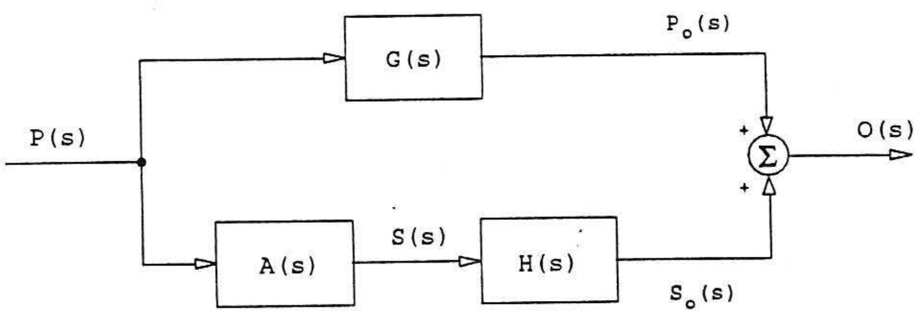

(c)

Fig. 2: Feedforward control structure;
(a) Schematic diagram,
(b), (c) Block diagram.

$E(s)$ = transfer function of path r_e,

$F(s)$ = transfer function of path r_f,

$G(s)$ = transfer function of path r_g,

$H(s)$ = transfer function of path r_h,

$M(s)$ = transfer function of the detector,

$C(s)$ = transfer function of the controller,

$N(s)$ = transfer function of necessary electronics,

$L(s)$ = transfer function of the secondary source.

From the block diagram in Fig. 2b the detector output $D(s)$ and secondary source output $S(s)$ are

$$D(s) = E(s)P(s) + F(s)S(s) \tag{3}$$

and

$$S(s) = M(s)C(s)N(s)L(s)D(s) \tag{4}$$

Substituting for $D(s)$ from equation (3) into equation (4) and simplifying yields the transfer function $A(s)$ between the secondary source and primary source outputs as

$$A(s) = \frac{S(s)}{P(s)} = \frac{M(s)C(s)N(s)L(s)E(s)}{1 - M(s)C(s)N(s)L(s)F(s)} \tag{5}$$

Thus, using $A(s)$ Fig. 2b can be represented in a simplified form as shown in Fig. 2c.

It follows from the block diagrams in Figs. 2b and 2c that, in the FFCS, the secondary path, i.e through $C(s)$ to the observation point, attempts to compensate the primary path, i.e. through $G(s)$ to the observation point, such that the superposition of the primary and secondary waves results in cancellation at and in the vicinity of the observation point.

As seen in Fig. 2a the detector gives a combined measure of the primary and secondary waves that reach the detection point through the acoustic paths r_e and r_f respectively. The secondary wave thus reaching the detector forms a closed feedback loop (Fig. 2b) that can cause the system to become unstable. Therefore, a careful consideration of this loop is necessary in the design stage. Alternative techniques attempting to avoid the instability problem in one-dimensional propagation (duct noise) by isolating the detector from secondary source radiation through using either uni-directional detectors or multiple-detector/multiple-source configurations such as acoustic dipole and tripole have been reported [14-17]. It is possible to avoid the instability problem in three-dimensional propagation by using uni-directional detector(s) or by employing indirect detection. However, a stability analysis of the system based on relative stability margins will lead to a robust design.

Note, in Fig. 2b, that moving the observation point so that to coincide with the detection point will lead to the FBCS of Fig. 1a. Therefore, in the subsequent developments the FFCS is given a relatively more detailed consideration, whereas, the FBCS is considered as a special case of the FFCS.

The FFCS corresponds to that proposed by Lueg in his patent where the time delay is implemented by the physical separation between the primary and secondary sources [5]. A significant amount of consideration has subsequently been given to this structure in various applications. Conover, Hesselman and Ross have employed this structure in the cancellation of transformer noise [18-21]. Ross has considered the design, Roure has analysed the stability, Eriksson, et.al. have considered the implementation of this structure in the cancellation of the one-dimensional duct noise [17, 22-26]. Nelson, et.al. have analysed the performance of this structure in the cancellation of enclosed sound fields [27-29]. Tokhi and Leitch have considered the design, performance and implementation of this structure in the cancellation of noise in three-dimensional propagation medium

[30-32].

3. Design of the controller

As stated earlier the controller in an ANC system requires a careful consideration in the design stage. The controller should be capable of altering the amplitude and phase of every frequency component of a detected primary wave properly. Moreover, as noted above, due to acoustic feedback from the secondary source radiation to the detector, stability conditions must be considered so that good system performance is ensured.

3.1. *Feedback control structure*

The objective in a FBCS (Fig. 1) is to reduce the detected signal to zero. Thus,

$$D(s) = 0 \tag{6}$$

This, using equation (2) and the Shwartz inequality, means that the following should hold [33]

$$| D(s) | \leq | 1 + M(s)C'(s)N(s)L(s)F(s) |^{-1} | E(s) | | P(s) | \tag{7}$$

Equation (7) implies that for a given detector, necessary electronics and secondary source the factor $| 1 + M(s)F(s)N(s)L(s)F(s) |^{-1}$ should tend to zero which in turn implies that $C'(s)$ or, equivalently, the controller transfer function $C(s)$ should have infinite amplitude;

$$| C(s) | = \infty \tag{8}$$

In practice this is not feasible as the transfer characteristics $M(s)$, $N(s)$, $L(s)$, $F(s)$ and $C(s)$ itself will induce instability in the loop. The maximum value of $| C(s) |$ can be determined from the Nyquist stability criterion, and for satisfactory operation a suitable stability margin is required. This represents a major limitation of the feedback control structure: to achieve good cancellation a high gain controller is required but this can lead to instability in the system. Therefore, in designing the controller the loop formed by $M(s)$, $C(s)$, $N(s)$, $L(s)$, $F(s)$ should be analysed and a compromise made between controller gain and system performance.

3.2. *Feedforward control structure*

The objective with the FFCS, Fig. 2, is to reduce the observed signal to zero. This requires that the observed primary and secondary signals should be equal in amplitude and opposite in phase; i.e

$$P_o(s) = -\, S_o(s) \tag{9}$$

From Fig. 2b the primary and secondary signals $P_o(s)$ and $S_o(s)$ are

$$\begin{aligned} P_o(s) &= G(s)P(s) \\ S_o(s) &= H(s)S(s) \end{aligned} \tag{10}$$

Substituting for $P_o(s)$ and $S_o(s)$ from equations (10) into equation (9), using equation (5), and simplifying yields

$$G(s) = -\, H(s)A(s) \tag{11}$$

Equation (11) is the required condition under which optimum cancellation is achieved in a stationary (steady-state) environment. Substituting for $A(s)$ from equation (5) into equation (11) and solving for $C(s)$ yields

$$C(s) = \frac{G(s)}{M(s)N(s)L(s)\Delta(s)} \tag{12}$$

where

$$\Delta(s) = F(s)G(s) - E(s)H(s) \tag{13}$$

Equation (12) represents the required controller transfer function for optimum cancellation of the unwanted noise over the frequency range of interest at steady state.

3.3. *Practical limitaions in the controller design*

It follows from equation (12) that for a particular detector and secondary source with necessary electronic components, the controller characteristics required for optimum (full) cancellation is dependent on the characteristics of the acoustic paths from the primary and secondary sources to the detector and observer locations. Any combination of the detector and observer locations with respect to the primary and secondary sources requires a particular controller characteristic. In particular, if the detector and observer are located such that $\Delta(s)$, equation (12), becomes zero then the critical situation of infinite gain controller requirement arises. The locus of such points in the medium (as a practical limitation in the design of the controller) is therefore of crucial interest.

3.3.1. Locus of the infinite–gain controller

If $\Delta(s)$ in equation (12) becomes zero then infinite gain is required of the controller. Under such a situation equation (13) for $s = j\omega$ yields

$$\frac{F(j\omega)}{E(j\omega)} = \frac{H(j\omega)}{G(j\omega)} \tag{14}$$

$E(j\omega)$, $F(j\omega)$, $G(j\omega)$ and $H(j\omega)$ are the frequency responses of the acoustic paths through the distances r_e, r_f, r_g and r_h respectively;

$$E(j\omega) = \frac{A}{r_e} e^{-j\frac{2\pi}{\lambda} r_e} \quad ; \quad F(j\omega) = \frac{A}{r_f} e^{-j\frac{2\pi}{\lambda} r_f}$$
$$G(j\omega) = \frac{A}{r_g} e^{-j\frac{2\pi}{\lambda} r_g} \quad ; \quad H(j\omega) = \frac{A}{r_h} e^{-j\frac{2\pi}{\lambda} r_h} \tag{15}$$

where λ is the signal wavelength, and A is a constant.

Substituting for $E(j\omega)$, $F(j\omega)$, $G(j\omega)$ and $H(j\omega)$ from equations (15) into equation (14) and simplifying yields

$$\left(\frac{r_e}{r_f}\right) e^{-j(r_f - r_e)\frac{2\pi}{\lambda}} = \left(\frac{r_g}{r_h}\right) e^{-j(r_h - r_g)\frac{2\pi}{\lambda}} \quad (16)$$

This equation is true if and only if the amplitudes as well as the exponents (phases) on either side of the equation are equal. Equating the amplitudes and the phases, accordingly, yields

$$\frac{r_e}{r_f} = \frac{r_g}{r_h} = a$$
$$r_f - r_e = r_h - r_g \quad (17)$$

where a, the distance ratio, is a positive real number.

Equations (17) define the locus of points for which $\Delta(j\omega) = 0$ and the controller is required to have an infinitely large gain. Note that these equations are in terms of the distances r_e, r_f, r_g and r_h only. Therefore, the critical situation of $\Delta(j\omega) = 0$ in a non-dispersive three-dimensional propagation medium is determined only by locations of the detector and observer relative to the primary and secondary sources.

Eliminating r_f and r_h in equations (17) and simplifying yields

$$r_e\,(a - 1) = r_g\,(a - 1) \quad (18)$$

Two possible situations, namely $a = 1$ and $a \neq 1$, are considered separately.

(i) Unity distance ratio

For a unity distance ratio, $a = 1$, equation (18) yields the identity $0 = 0$. Therefore, substituting for $a = 1$ into equations (17) yields the locus of points for which infinite gain is required of the controller as

$$\frac{r_e}{r_f} = 1 \quad \text{and} \quad \frac{r_g}{r_h} = 1 \tag{19}$$

If the locations of the primary and secondary sources are fixed then each of equations (19) defines a surface plane perpendicularly bisecting the line joining the primary and secondary source locations (see Appendix A). This plane for the primary and secondary sources respectively located at points (0, 0, 0) and (u_s , v_s , w_s) with a distance d apart in a three-dimensional UVW–space (see Fig. 3) is given by

$$\frac{u}{\left(\frac{d^2}{2u_s}\right)} + \frac{v}{\left(\frac{d^2}{2v_s}\right)} + \frac{w}{\left(\frac{d^2}{2w_s}\right)} = 1 \tag{20}$$

which intersects the U–, V–, and W–axes respectively at points $(\frac{d^2}{2u_s}, 0, 0)$, $(0, \frac{d^2}{2v_s}, 0)$, and $(0, 0, \frac{d^2}{2w_s})$. This plane is shown in Fig. 4. If the detector is placed at any point on this plane and if at the same time the observer location coincides with a point on this plane then the 'critical situation' of equation (14) occurs and the controller is required to have an infinitely large gain.

(ii) Non unity distance ratio

For a non-unity distance ratio, $a \neq 1$, equations (17) and (18) yield the locus of points for which an infinitely large gain is required of the controller as

$$\frac{r_e}{r_f} = a \ , \quad \frac{r_g}{r_h} = a \quad \text{and} \quad \frac{r_e}{r_g} = 1 \tag{21}$$

It follows from Appendix A that the first two relations in equations (21) each define a spherical surface. These surfaces for the primary and secondary sources located as in Fig. 3 are defined by

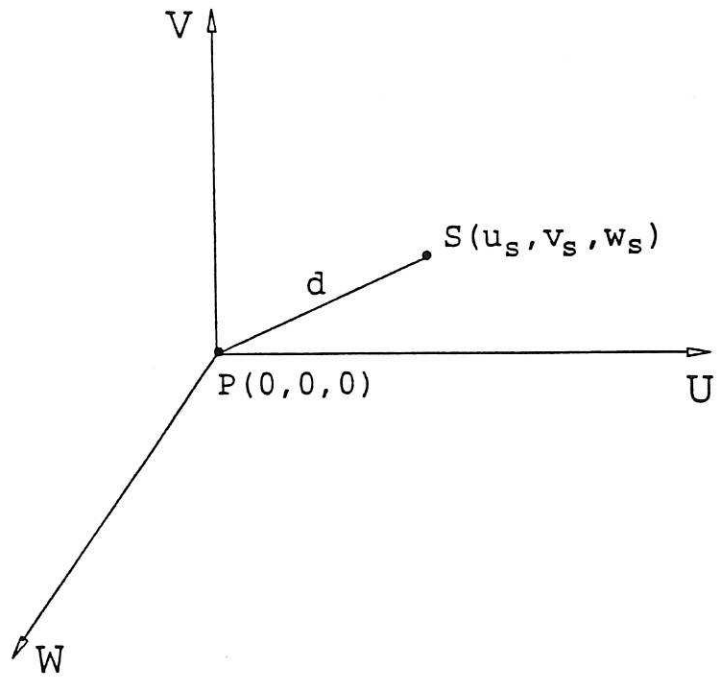

Fig. 3: Primary and secondary sources
in three-dimensional coordinates.

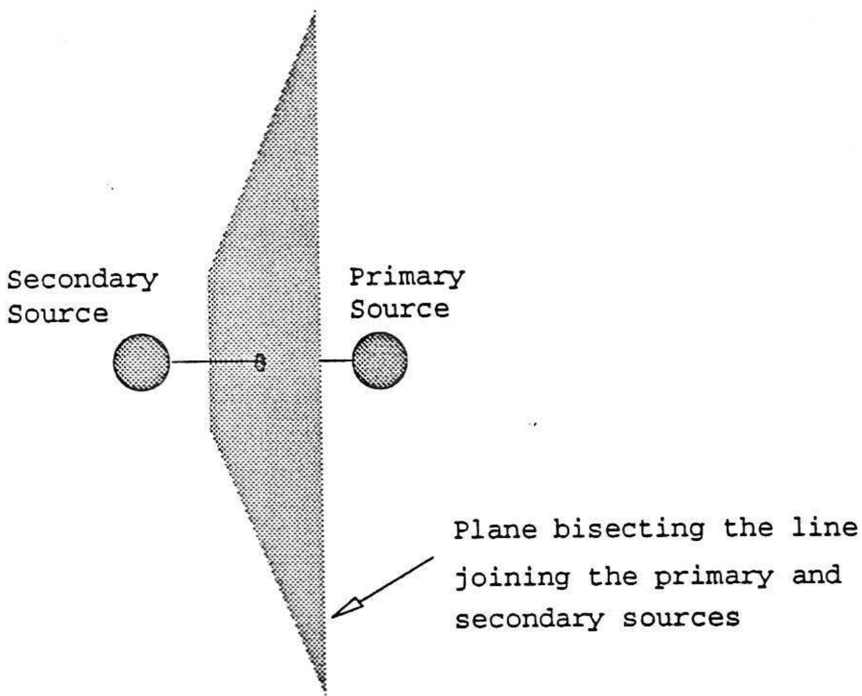

Fig. 4: Plane of the infinite-gain controller.

$$\left[u + \frac{a^2 u_s}{1 - a^2} \right]^2 + \left[v + \frac{a^2 v_s}{1 - a^2} \right]^2 + \left[w + \frac{a^2 w_s}{1 - a^2} \right]^2 = \left[\frac{ad}{1 - a^2} \right]^2 \qquad (22)$$

which has a radius $R = \dfrac{ad}{|1 - a^2|}$ and centre located along the line PS, joining the primary and secondary source locations, at the point $Q\ (-\dfrac{a^2 u_s}{1 - a^2}, -\dfrac{a^2 v_s}{1 - a^2}, -\dfrac{a^2 w_s}{1 - a^2})$. This is shown in two dimensions in Fig. 5 which implies that both the detector and the observer locations should coincide with points on this sphere.

The third relation in equation (21) requires the equality of the distances between the detector and primary source (r_e) and between the observer and primary source (r_g). The locus of such points in the three-dimensional UVW–space of Fig. 3 (for, say, constant r_e) is a sphere with centre at the primary source location and radius equal to r_e;

$$u^2 + v^2 + w^2 = r_e^{\,2} \qquad (23)$$

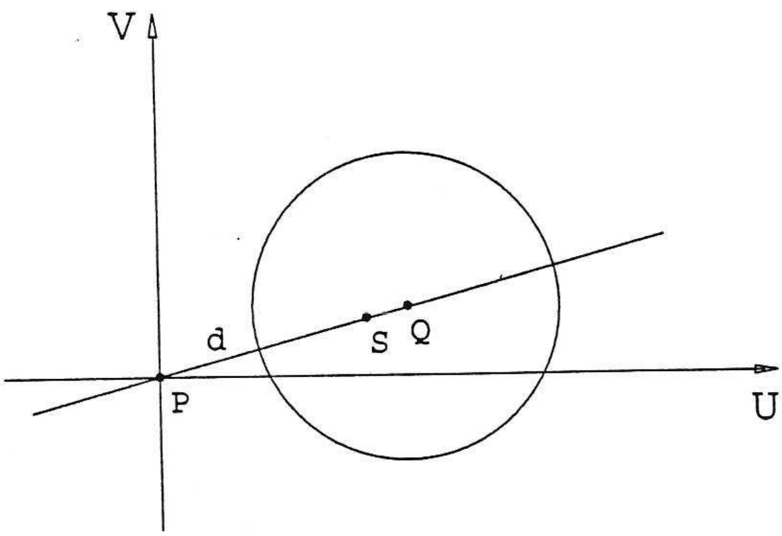

Fig. 5: Locus of constant distance ratio.

This is shown in the two dimensions in Fig. 6. Therefore, the locus of points defined by equations (21) is given by the intersection of the two spheres in equations (22) and (23). Such an intersection results a circle, hereafter referred to as the infinite gain controller (IGC) circle, located in a plane that is at right angles with the line joining the centres of the spheres. The centre of the circle is the point of intersection of the plane and the line.

To investigate the variation of the IGC circle in terms of its radius and location of its centre in the three-dimensional *UVW*–space of Fig. 3, let the detector be located at point *E* with coordinates (u_e, v_e, w_e) and distances r_e and r_f relative to the primary and secondary sources respectively, as shown in Fig. 7. Substituting for $u^2 + v^2 + w^2$ from equation (23) into equation (22) and simplifying yields the plane of the IGC circle as

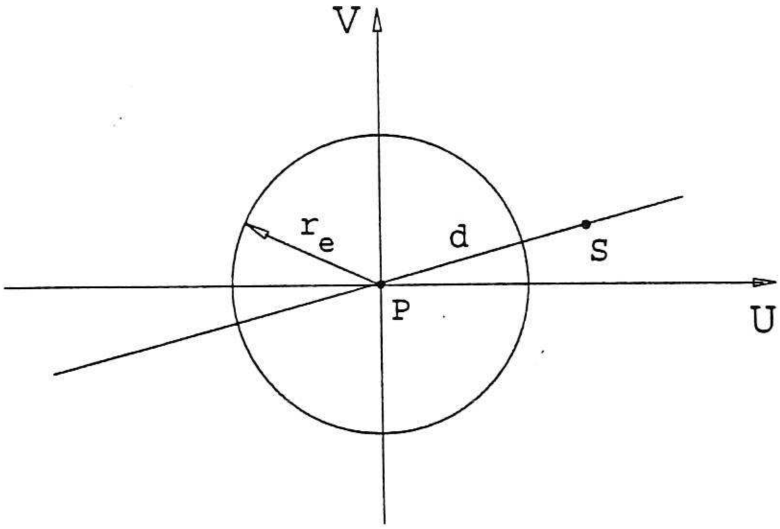

Fig. 6: Locus of points $r_e = r_g$.

$$\frac{u}{\left(\frac{B}{u_s}\right)} + \frac{v}{\left(\frac{B}{v_s}\right)} + \frac{w}{\left(\frac{B}{w_s}\right)} = 1 \qquad (24)$$

where

$$B = \frac{1}{2}\left[d^2 - \left(\frac{1}{a^2} - 1\right) r_e^2\right] = \frac{1}{2}\left[d^2 - (r_f^2 - r_e^2)\right] \qquad (25)$$

Equation (24) defines a plane surface on which the IGC circle is residing. In accordance to the procedure described in Appendix A it is found that the line *PS* passing through the primary and secondary source locations is at right angles with the plane of IGC circle. This is shown in two dimensions in Fig. 8a. The corresponding IGC circle is shown in Fig. 8b where r_c is the radius of the IGC circle.

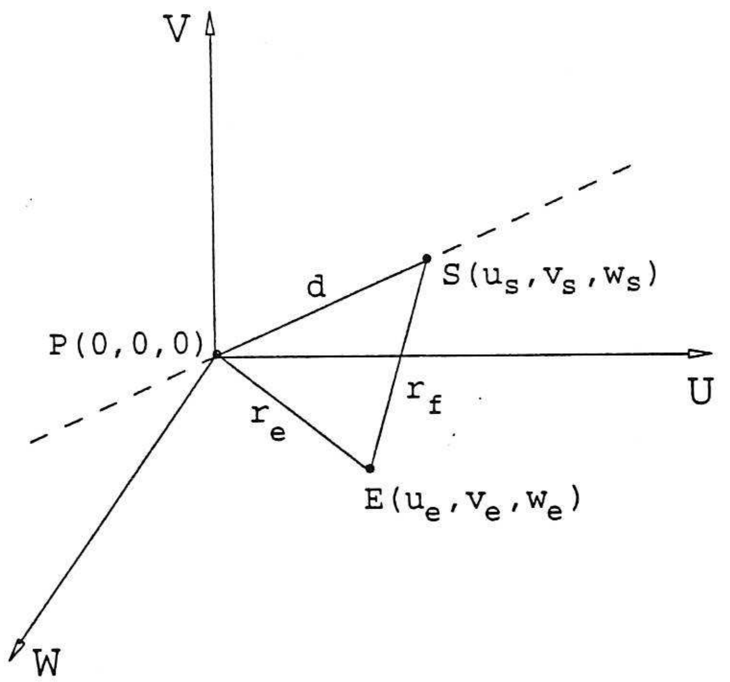

Fig. 7: Location of detector relative to primary and secondary sources.

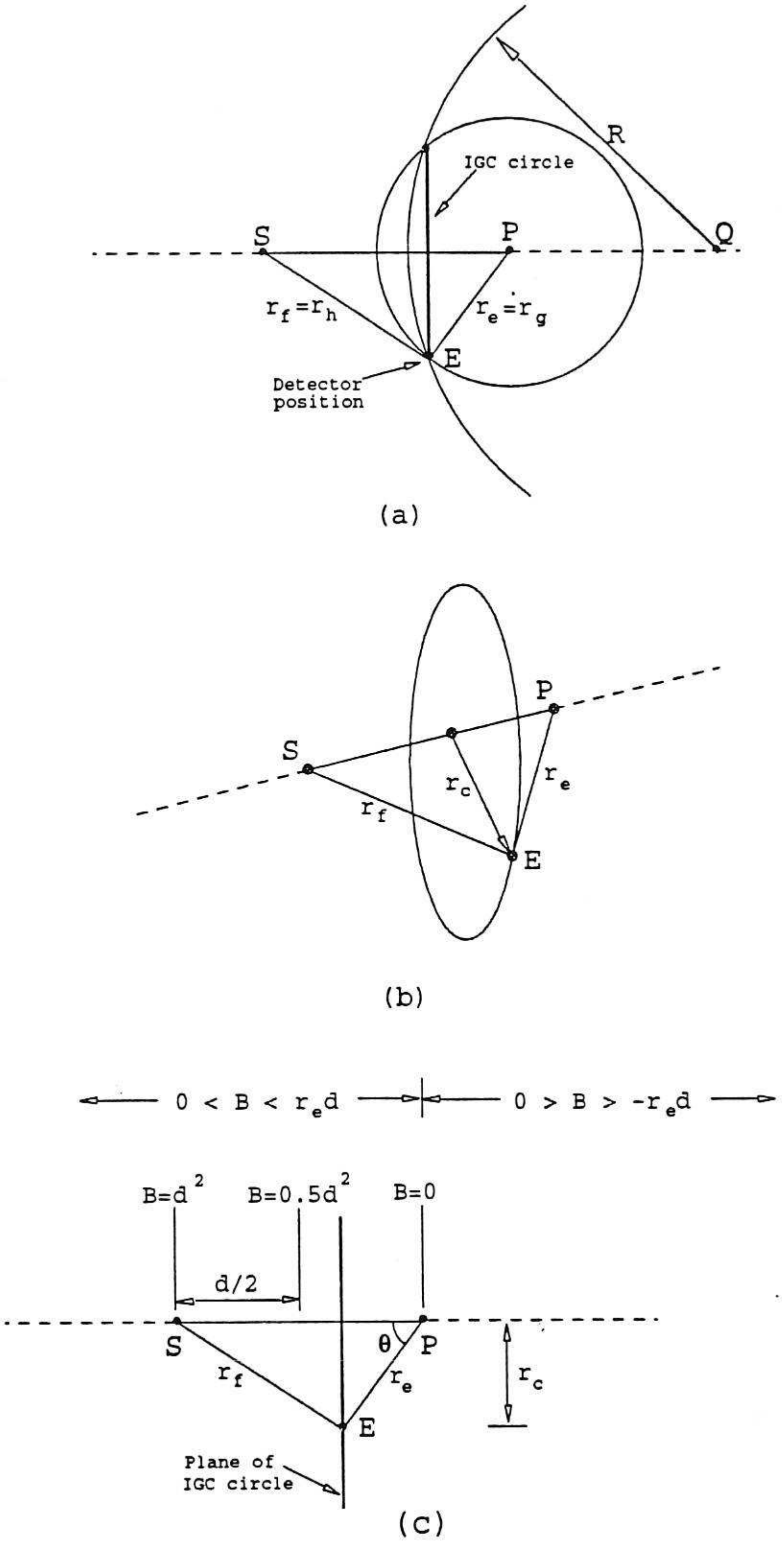

Fig. 8: The infinite-gain controller circle;

(a) Formation,

(b) IGC circle,

(c) Position with detector location.

The quantity B in equation (25) gives a measure of the intersection of the plane in equation (24) with the coordinate axes and, thereby, with the line PS passing through locations of the primary and secondary sources. It is evident from equation (25) that B is dependent on d, r_e and r_f or, for constant d, is dependent on location of detector only. If θ denotes the angle between the lines PE and PS in a plane formed by these lines (Fig. 8c) then the following holds

$$r_f^2 = d^2 + r_e^2 - 2r_e d\cos\theta \tag{26}$$

Substituting for r_f^2 from equation (26) into equation (25) yields

$$B = r_e d\cos\theta \tag{27}$$

Therefore, as the detection point changes position in the medium the limits for B are found to be

$$| B | < r_e d \tag{28}$$

This variation, in relation to the location of the plane of IGC circle, is shown in two dimensions in Fig. 8c. For $r_f^2 - r_e^2 > d^2$, in which case $0 > B > -r_e d$, the plane passes through points along the line PS which are outside the range (P, S) and their distances from P are smaller than those from point S. As $r_f^2 - r_e^2$ decreases the plane moves towards point P. At point P where $r_f^2 - r_e^2 = d^2$ the quantity B is zero. If $r_f^2 - r_e^2$ is further decreased so that a is still less than unity the plane moves towards the midpoint between P and S. Midway between P and S the distance ratio a is unity ($r_f = r_e$), $B = \frac{1}{2} d^2$ and the plane coincides with the plane in equation (20), (Fig. 4). After the point midway between P and S ($a > 1$) as the distance ratio a is increased the plane moves towards point S and further beyond it. At point S where $r_e^2 - r_f^2 = d^2$ the quantity B is equal to d^2.

From Fig. 8c the radius r_c of the IGC circle can be written as

$$r_c = r_e \sin\theta \quad ; \quad 0 \leq \theta \leq \pi \tag{29}$$

Thus, the radius of the IGC circle is dependent on the distance r_e between the primary source and the detector and the sine of the angle formed by the line joining the primary source and detector with the line joining the primary and secondary sources. The maximum value of the radius, $r_{c\,\max}$, is r_e and occurs at the situation where the plane of IGC circle intersects the line *PS* at point *P* (Fig. 8c);

$$r_{c\,\max} = r_e \tag{30}$$

Movement of the plane to either side of point *P* will lead to a decrease in the radius. At the extreme cases where the line *PE* is in alignment with the line *PS* (θ is either 0° or 180°) the radius r_c is zero. In general, for constant values of the angle θ the radius r_c is directly proportional to the distance r_e between the primary source and the detector. This implies that in order for r_c to be minimised the detector is required to be placed as close to the primary source as possible.

It follows from the above that the requirement of an infinitely large gain controller in a FFCS is directly linked with the locations of the detector and observer relative to the primary and secondary sources. This derives from the dependence of the controller characteristics on the transfer characteristics of the acoustic paths from the detector and observer to the primary and secondary sources which demand a particular controller transfer function for a particular combination of the detector and observer locations in the medium. The above analysis reveals that combinations of the detector and observer locations in the medium exist that for optimum cancellation require the controller to have an infinitely large gain. These form the locus of infinite gain controller requirement which are:

(*a*) If the detector and observer are equidistant from the sources the locus is a plane surface that perpendicularly bisects the line joining the locations of the primary and secondary sources.

(*b*) If the detector and observer are not equidistant from the sources the locus is a circle, with centre along the line joining the locations of the primary and secondary sources, and on a plane that is parallel with that in (*a*). The radius of the circle is given by the distance between the detector and the line.

Note in equation (21) that if the first two of the relations are divided side-by-side (assuming $a \neq 0$) then the following equivalent equations are obtained

$$\frac{r_e}{r_g} = 1 \quad \text{and} \quad \frac{r_f}{r_h} = 1 \qquad (31)$$

This means that starting with equations (31), rather than equation (21), will also lead to exactly the same results obtained in the preceding paragraphs.

The crucial situation of infinite-gain controller requirement was shown in the above, on the basis of using omni-directional sensors and sources, to exist with the general ANC structure. The problem can be avoided by confining the detector and observer to regions of the medium that are outside the loci in (*a*) and (*b*) above. A further possibility of avoiding this problem is to isolate the detector from secondary source radiation. A method of achieving this is to use a uni-directional detector such that it is subjected to the primary wave only. Alternatively, indirect detection, as discussed earlier, can be used. Either of these methods, in terms of the FFCS of Fig. 2, are equivalent to making $F(s) = 0$, under which the controller transfer function in equation (12) becomes

$$C(s) = -\frac{G(s)}{M(s)N(s)L(s)E(s)H(s)} \quad \text{for} \quad F(s) = 0 \qquad (32)$$

The use of uni-directional microphones as an attempt to avoid the infinite-gain controller requirement has be considered by Roure in the case of one-dimensional propagation (duct noise) [17]. Others have reported alternative configurations of multiple-detector/ multiple-source for the one-dimensional duct noise problem as attempts at isolating the detector from secondary source radiation [14-16].

3.3.2. Feedback control structure

As noted earlier, if the observer in a FFCS shown in Fig. 2a moves to coincide with the detector then the FBCS is obtained. In such a process the distances r_g and r_h are effectively made to approach the distances r_e and r_f, respectively. This in terms of the transfer functions $E(s)$, $F(s)$, $G(s)$ and $H(s)$ leads to

$$\begin{aligned} G(s) &= E(s) \\ H(s) &= F(s) \end{aligned} \tag{33}$$

Projecting the above modifications into the controller design equations of a FFCS the corresponding controller design equations for the FBCS are obtained.

Substituting for $G(s)$ and $H(s)$ from equations (33) into equation (13) and simplifying yields

$$\Delta(s) = 0 \tag{34}$$

Equation (34) corresponds to the critical situation of impractically large-gain controller requirement discussed above. Therefore, as also derived earlier from a different perspective, for optimum cancellation of the noise the FBCS will always require a controller with an infinitely large gain. With a practically acceptable compromise between system performance and controller gain, and careful consideration of the stability of the system, reasonable amounts of cancellation of the noise can be achieved with this structure.

4. Conclusion

An analysis and design procedure for ANC systems in a three-dimensional non-dispersive propagation medium has been presented.

The optimum cancellation of an unwanted noise in three dimensions requires a controller with a frequency-dependent transfer function that can produce a wave which is an exact mirror image of the noise so that when superimposed on the noise results in silence. The characteristics of such a controller are found to be dependent upon the transfer characteristics of transducers, secondary source and propagation paths from the primary and secondary sources to both the detector and observer locations.

The dependence of controller characteristics on the characteristics of system components and geometry can sometimes lead to practical difficulties in the controller design and system stability. A particular combination of these characteristics requires a controller of a particular transfer function. A change in any of these characteristics, such as changing the location of either the detector and/or observer, requires a controller with a new transfer function to suit the new situation. In particular there are combinations of detector and observer locations which lead to the critical situation of infinite-gain controller requirement. Two situations in general lead to the IGC requirement

(*i*) When both the observer and detector are equidistant from the primary and secondary sources. In a FBCS, where both the detection and observation points are the same, this situation corresponds to the detector being on a plane that perpendicularly bisects the line joining the locations of the sources. In a FFCS this situation corresponds to when both the detector and observer are on this plane.

(*ii*) When the ratio of the distances from detector and observer to primary source and ratio of distances from detector and observer to secondary source are each equal to unity; i.e. the detector and observer are both on a circle (the IGC circle) which is in a plane that makes a 90 degrees angle with the line passing through locations of primary and secondary sources. In a FBCS where the detector and observer are both located at the same point this situation of IGC requirement is always satisfied. In a FFCS, however, it is possible to minimise the region of space occupied by the IGC circle by a proper geometrical arrangement of system components.

5. References

1. KIM, C. D., MORIKAWA, S., ABE, M., and KIDO, K.: 'Active suppression of noise in microphone line using vibration of noise source', Proceedings of Inter-noise 84, 1984, **I**, pp. 469-472
2. DINES, P. J.: 'Comparison of least squares estimation and impulse response techniques for active control of flame noise', Proceedings of the Institute of Acoustics, November 1982, pp. F2.1-F2.4
3. ROSS, C. F.: 'Quietening newspaper printing presses by active control', Proceedings of the Institute of Acoustics, November 1982, pp. F1.1-F1.4
4. ROSS, C. F.: 'Novel applications of active control techniques', Proceedings of the Institute of Acoustics, 1986, **8**(Part 1), pp. 127-133
5. LUEG, P.: 'Process of silencing sound oscillations', U.S. Patent No. 2 043 416, 1936
6. OLSON, H. F. and MAY, E. G.: 'Electronic sound absorbers', Journal of the Acoustical Society of America, 1953, **25**, pp. 1130-1136
7. OLSON, H. F.: 'Electronic control of noise, vibration and reverberation', Journal of the Acoustical Society of America, 1956, **28**, pp. 966-972
8. OLSON, H. F.: 'Electronic sound absorber', U.S. Patent No. 2 983 790, 1961

9. BLEAZY, J. C.: 'Electronic sound absorber', Journal of Audio Engineering Society, 1962, **10**, (2), pp. 135-139

10. SHORT, W. R.: 'Global low frequency active noise attenuation', Proceedings of Inter-noise 80, 1980, **II**, pp. 695-698

11. TRINDER, M. C. J. and NELSON, P. A.: 'The acoustical virtual earth and its application to ducts with reflecting terminations', Proceedings of Inter-noise 83, 1983, **I**, pp. 447-450

12. TRINDR, M. C. J. and NELSON, P. A.: 'Active noise control in finite length ducts', Journal of Sound and Vibration, 1983, **89**, (1), pp. 95-106

13. CHAPLIN, G. B. B., JONES, A., and JONES, O.: 'Method and apparatus for low frequency active attenuation', U.S. Patent No. 4 527 282, 1985

14. JESSEL, M. and MANGIANTE, G. A.: 'Active sound absorbers in an air duct', Journal of Sound and Vibration, 1972, **23**, (3), pp. 383-390

15. SWINBANKS, M. A.: 'Active control of sound propagation in long ducts', Journal of Sound and Vibration, 1973, **27**, (3), pp. 411-436

16. LEVENTHAL, H. G. and EGHTESADI, Kh.: 'Active attenuation of noise: Monopole and Dipole systems', Proceedings of Inter-noise 79, 1979, **I**, pp. 175-180

17. ROURE, A.: 'Self-adaptive broadband active sound control system', Journal of Sound and Vibration, 1985, **101**, (3), pp. 429-441

18. CONOVER, W. B.: 'Fighting noise with noise', Noise Control, 1956, **92**, pp. 78-82 & 92

19. CONOVER, W. B.: 'Noise reducing system for transformers', U.S. Patent No. 2 776 020, 1957

20. HESSELMAN, N.: 'Investigation of noise reduction on a 100 KVA transformer tank

by means of active methods', Applied Acoustics, 1978, **11**, (1), pp. 27-34

21. ROSS, C. F.: 'Experiments on the active control of transformer noise', Journal of Sound and Vibration, 1978, **61**, (4), pp. 473-480

22. ROSS, C. F.: 'Design of a broadband active sound control system', Proceedings of the Institute of Acoustics, 1981, pp. 21-24

23. ERIKSSON, L. J., ALLIE, M. C., and GREINER, R. A.: 'The selection and application of an IIR adaptive filter for use in active sound attenuation', IEEE Transactions on Acoustics, Speech, and Signal Processing, 1987, **ASSP–35**, (4), pp. 433-437

24. MUNJAL, M. L. and ERIKSSON, L. J.: 'An analytical, one-dimensional, standing-wave model of a linear active noise control system in a duct', The Journal of the Acoustical Society of America, 1988, **84**, (3), pp. 1086-1093

25. ERIKSSON, L. J., ALLIE, M. C., BREMIGAN, C. D., and GREINER, R. A.: 'Active noise control using adaptive digital signal processing', Proceedings of the IEEE International Conference on Acoustics, Speech, and Signal Processing, 1988, **5**, pp. 2594-2597

26. ERIKSSON, L. J., ALLIE, M. C., BREMIGAN, C. D., and GILBERT, J. A.: 'Active noise control and specifications for fan noise problems', Proceedings of Noise-Con 88, 1988, pp. 273-278

27. NELSON, P. A., CURTIS, A. R. D., ELLIOTT, S. J., and BULLMORE, A. J.: 'The active minimization of harmonic enclosed sound fields, Part I: Theory', Journal of Sound and Vibration, 1987, **117**, (1), pp. 1-13

28. BULLMORE, A. J., NELSON, P. A., CURTIS, A. R. D., and ELLIOTT, S. J.: 'The active minimization of harmonic enclosed sound fields, Part II: A computer simulation', Journal of Sound and Vibration, 1987, **117**, (1), pp. 15-33

29. ELLIOTT, S. J., CURTIS, A. R. D., BULLMORE, A. J., and NELSON, P. A.: 'The active minimization of harmonic enclosed sound fields, Part III: Experimental verification', Journal of Sound and Vibration, 1987, **117**, (1), pp. 35-58

30. LEITCH, R. R. and TOKHI, M. O.: 'The implementation of active noise control systems using digital signal processing techniques', Proceedings of the Institute of Acoustics, 1986, **8**, (Part 1), pp. 149-157

31. LEITCH, R. R. and TOKHI, M. O.: 'Active noise control systems', IEE Proceedings, Part A, 1987, **134**, (6), pp. 525-546

32. TOKHI, M. O. and LEITCH, R. R.: 'Self-tuning active noise control', IEE Colloquium on Adaptive Filters, 1989

33. TROPPER, A. M.: 'Linear Algebra', 1969, Nelson, U.K.

Appendix A: Locus of constant distance ratio

Theorem A

Let P and S be two fixed points in a three-dimensional space with a distance d apart from each other and let T be an arbitrary point in this space. If the ratio of the distances PT and ST is constant then the locus of points T defines

(*a*) a sphere with centre located along the line PS, for a non-unity distance ratio.

(*b*) a plane perpendicularly bisecting the line joining the points P and S, for a unity distance ratio.

Proof:

Consider the three-dimensional *UVW*–space of Fig. A.1 in which $P(0, 0, 0)$ and

$S\ (u_s, v_s, w_s)$ represent two fixed points and $T\ (u, v, w)$ an arbitrary point. The distances PS, PT and ST are respectively denoted by d, r_g and r_h. Let the distance ratio $\frac{r_g}{r_h}$ be denoted by, a positive real number, a;

$$\frac{r_g}{r_h} = a \qquad \text{(A.1)}$$

It follows from Fig. A.1 that

$$d = \left[u_s^2 + v_s^2 + w_s^2 \right]^{\frac{1}{2}} \qquad \text{(A.2)}$$

$$r_g = \left[u^2 + v^2 + w^2 \right]^{\frac{1}{2}}$$

$$r_h = \left[(u - u_s)^2 + (v - v_s)^2 + (w - w_s)^2 \right]^{\frac{1}{2}} \qquad \text{(A.3)}$$

Substituting for r_g and r_h from equations (A.3) into equation (A.1), simplifying and using equation (A.2) yields

$$(1 - a^2)\, u^2 + 2\, a^2\, u_s u + (1 - a^2)\, v^2 + 2\, a^2\, v_s v + (1 - a^2)\, w^2 + 2\, a^2\, w_s w = a^2\, d^2 \qquad \text{(A.4)}$$

This gives the locus of points in the three-dimensional UVW–space that corresponds to a particular distance ratio a.

(i) Non–unity distance ratio

If the distance ratio a is different from unity then equation (A.4), after completing squares and simplifying, yields

$$\left[u + \frac{a^2\, u_s}{1 - a^2} \right]^2 + \left[v + \frac{a^2\, v_s}{1 - a^2} \right]^2 + \left[w + \frac{a^2\, w_s}{1 - a^2} \right]^2 = \left[\frac{ad}{1 - a^2} \right]^2 \quad , \; a \neq 1 \qquad \text{(A.5)}$$

This equation represents a sphere with radius $R = \frac{ad}{|1 - a^2|}$ and centre at $Q\,(-\frac{a^2 u_s}{1 - a^2}, -\frac{a^2 v_s}{1 - a^2}, -\frac{a^2 w_s}{1 - a^2}\,)$.

In order to prove that the centre of the sphere Q is located along the line PS let the coordinates of this point be denoted by (u_q, v_q, w_q), unit vectors in the directions of U, V and W axes respectively be denoted by i, j, and k and a unit vector along some line AB pointing towards point B be denoted by I_{ab}. Thus,

$$u_q = -\frac{a^2 u_s}{1 - a^2}$$
$$v_q = -\frac{a^2 v_s}{1 - a^2} \qquad \text{(A.6)}$$
$$w_q = -\frac{a^2 w_s}{1 - a^2}$$

and

$$I_{ps} = \frac{u_s\, i + v_s\, j + w_s\, k}{\sqrt{u_s^2 + v_s^2 + w_s^2}}$$
$$\qquad \text{(A.7)}$$
$$I_{pq} = \frac{u_q\, i + v_q\, j + w_q\, k}{\sqrt{u_q^2 + v_q^2 + w_q^2}}$$

Substituting for u_q, v_q and w_q from equations (A.6) into equation (A.7), simplifying and using equation (A.2) yields

$$I_{ps} = \frac{1}{d}\,(u_s\, i + v_s\, j + w_s\, k)$$
$$\qquad \text{(A.8)}$$
$$I_{pq} = -\frac{|1 - a^2|}{1 - a^2}\,\frac{1}{d}\,(u_s\, i + v_s\, j + w_s\, k)$$

which implies that

$$I_{pq} = \begin{cases} +\, I_{ps} & \text{for } a > 1 \\ -\, I_{ps} & \text{for } a < 1 \end{cases} \tag{A.9}$$

It follows from equations (A.9) that the centre of the sphere Q is located along the line PS and, specifically, if P is chosen as reference then for $a > 1$ the centre is located on the portion of PS corresponding to points away from P in the direction of I_{ps} whereas for $a < 1$ the centre of the sphere will be on the portion of PS corresponding to points away from P in the direction of $-I_{ps}$. In either of these situations, as follows from equation (A.6), the centre of the sphere lies outside the range (P, S). This is proved as follows

Let the distance between points P and Q be denoted by r_{pq} and that between points Q and S be denoted by r_{sq}; thus

$$r_{pq} = \sqrt{u_q^2 + v_q^2 + w_q^2}$$

$$r_{sq} = \sqrt{(u_q - u_s)^2 + (v_q - v_s)^2 + (w_q - w_s)^2}$$

Substituting for u_q, v_q and w_q from equations (A.6) into the above, using equation (A.2) and simplifying yields

$$r_{pq} = \frac{a^2 d}{|1 - a^2|} \qquad r_{sq} = \frac{d}{|1 - a^2|} \tag{A.10}$$

from which it follows that

$$r_{pq} > r_{sq} \quad \text{and} \quad r_{pq} > d \quad \text{for } a > 1$$

$$r_{pq} < r_{sq} \quad \text{and} \quad r_{sq} > d \quad \text{for } a < 1$$

This proves that Q is always outside the range (P, S).

Let the line passing through points P and S intersect the sphere in equation (A.5) at point N (u_n, v_n, w_n) with distances r_{pn} and r_{sn}, respectively, relative to points P and S and let the unit vectors pointing towards N, respectively, from points P and S be I_{pn} and I_{sn}; thus

$$r_{pn} = \sqrt{u_n^2 + v_n^2 + w_n^2}$$
$$r_{sn} = \sqrt{(u_n - u_s)^2 + (v_n - v_s)^2 + (w_n - w_s)^2} \tag{A.11}$$

and

$$I_{pn} = \frac{u_n\, i + v_n\, j + w_n\, k}{r_{pn}}$$
$$I_{sn} = \frac{(u_n - u_s)\, i + (v_n - v_s)\, j + (w_n - w_s)\, k}{r_{sn}} \tag{A.12}$$

Since N is a point along the line PS the vectors I_{pn} and I_{sn} are either pointing to the same direction or in opposite directions. Thus, it follows from equations (A.12) that

$$\frac{| u_n |}{r_{pn}} = \frac{| u_n - u_s |}{r_{sn}}$$
$$\frac{| v_n |}{r_{pn}} = \frac{| v_n - v_s |}{r_{sn}} \tag{A.13}$$
$$\frac{| w_n |}{r_{pn}} = \frac{| w_n - w_s |}{r_{sn}}$$

Since $\frac{r_{pn}}{r_{sn}}$ represent the distance ratio a, equation (A.1), equations (A.13) can be written as

$$u_n^2 = a^2 (u_n - u_s)^2$$
$$v_n^2 = a^2 (v_n - v_s)^2 \tag{A.14}$$
$$w_n^2 = a^2 (w_n - w_s)^2$$

Solving the above for u_n, v_n and w_n yield

$$u_n = \left(\frac{-a^2 \pm a}{1-a^2} \right) u_s$$

$$v_n = \left(\frac{-a^2 \pm a}{1-a^2} \right) v_s \qquad \text{(A.15)}$$

$$w_n = \left(\frac{-a^2 \pm a}{1-a^2} \right) w_s$$

It follows from equations (A.15) that the line passing through points P and S and the sphere in equation (A.5) intersect at two points E and F with coordinates (u_e, v_e, w_e) and (u_f, v_f, w_f) respectively;

$$u_e = \frac{a}{1+a} u_s$$

$$v_e = \frac{a}{1+a} v_s \qquad \text{(A.16)}$$

$$w_e = \frac{a}{1+a} w_s$$

and

$$u_f = -\frac{a}{1-a} u_s$$

$$v_f = -\frac{a}{1-a} v_s \qquad \text{(A.17)}$$

$$w_f = -\frac{a}{1-a} w_s$$

Equations (A.16) and (A.17) imply that E is a point that is always located inside the range (P, S) and F outside this range. In particular, if $a > 1$ points E and F are nearer to point S whereas if $a < 1$ then points E and F are nearer to point P. If the distances from points E and F respectively to points P and S are denoted by r_{pe}, r_{se} and r_{pf}, r_{sf} then using equations (A.2), (A.16) and (A.17) these are

$$r_{pe} = \frac{a\,d}{1 + a}$$
$$r_{se} = \frac{d}{1 + a} \quad \text{(A.18)}$$

and

$$r_{pf} = \frac{a\,d}{|\,1 - a\,|}$$
$$r_{sf} = \frac{d}{|\,1 - a\,|} \quad \text{(A.19)}$$

(ii) Unity distance ratio

If $a = 1$ then equation (A.1) yields

$$r_g = r_h \quad \text{(A.20)}$$

Substituting for r_g and r_h from equations (A.3) into equation (A.20), simplifying and using equation (A.2) yields

$$\frac{u}{\left(\frac{d^2}{2u_s}\right)} + \frac{v}{\left(\frac{d^2}{2v_s}\right)} + \frac{w}{\left(\frac{d^2}{2w_s}\right)} = 1 \quad \text{(A.21)}$$

This represents a plane surface which intersects the U, V and W axes, respectively, at the points $(\frac{d^2}{2u_s}, 0, 0)$, $(0, \frac{d^2}{2v_s}, 0)$, and $(0, 0, \frac{d^2}{2w_s})$.

The direction of the plane (A.21) is represented by a unit vector at right angle to the surface and pointing outward from the surface. Let such a unit vector be denoted by I_s. Simplifying equation (A.21) yields

$$2\,u_s\,u + 2\,v_s\,v + 2\,w_s\,w - d^2 = 0$$

Let the left-hand side of the above equation be denoted by some variable Z;

$$Z = 2\, u_s\, u + 2\, v_s\, v + 2\, w_s\, w - d^2 \tag{A.22}$$

So that as Z varies from $-\infty$ to $+\infty$ equation (A.22) defines an infinite set of plane surfaces parallel to the plane in equation (A.21), thus the unit vector I_s is given by

$$I_s = \frac{\frac{\partial Z}{\partial u}\, i + \frac{\partial Z}{\partial v}\, j + \frac{\partial Z}{\partial w}\, k}{\sqrt{\left[\frac{\partial Z}{\partial u}\right]^2 + \left[\frac{\partial Z}{\partial v}\right]^2 + \left[\frac{\partial Z}{\partial w}\right]^2}} \tag{A.23}$$

where $\frac{\partial}{\partial u}$, $\frac{\partial}{\partial v}$ and $\frac{\partial}{\partial w}$ respectively denote the partial derivatives with respect to u, v and w. Substituting for Z from equation (A.22) into equation (A.23), simplifying and using equation (A.2) yields

$$I_s = \frac{u_s}{d}\, i + \frac{v_s}{d}\, j + \frac{w_s}{d}\, k \tag{A.24}$$

comparison of which with equations (A.8) gives

$$I_s = I_{ps} \tag{A.25}$$

Equation (A.25) implies that the line PS is perpendicular to the plane surface in equation (A.21). Moreover, it follows from equation (A.20) that the point of intersection of the plane surface and the line PS is equidistant from points P and S. Therefore, the plane in equation (A.21) perpendicularly bisects the line PS.

Corollary A

Let P and S be two fixed points in a two-dimensional UV–space with a distance d apart from one another and let T be an arbitrary point in this space. If the ratio of the distances PT and ST is constant then the locus of points T defines

(*a*) a circle with centre located along the line PS, for a non-unity distance ratio.

$w_s = 0$ gives coordinates of the point of intersection of the two lines as $(\frac{u_s}{2}, \frac{v_s}{2})$ the distance of which from point P is found to be equal to $\frac{d}{2}$, i.e. midway between points P and S. The slopes m_1 and m_2 respectively of the lines in equations (A.27) and (A.28) are

$$m_1 = -\frac{u_s}{v_s}$$

$$m_2 = +\frac{v_s}{u_s}$$

i.e.

$$m_1 = -\frac{1}{m_2}$$

which implies that the two lines make a 90° angle at their point of intersection. Therefore, the line in equation (A.27) perpendicularly bisects the line PS.